INTERMEDIATE TO VERY HIGH STRAIN RATE BEHAVIOUR OF ALUMINIUM ALLOYS

Ljiljana DJAPIC OOSTERKAMP*, Trond FURU, Hans Erik VATNE**, Alojz IVANKOVIC*****

* R&D Materials Technology, Hydro Aluminium, N-4265 Håvik, Norway
** R&D Materials Technology, Hydro Aluminium, N-6601 Sunndalsøra, Norway
*** Imperial College, Mechanical Eng. Dep., Exhibition Road, London SW7 2BX, UK

ABSTRACT There is a long standing debate whether aluminium alloys exhibit high strain rate sensitivity. This paper aims at determination of the nature of the strain rate sensitivity of two aluminium alloys of 6xxx and 7xxx series in the as-extruded and tempered condition. Testing has been performed in simple (uniaxial) compression in the direction of extrusion. Computer-controlled servo hydraulic machine was used for intermediate strain rates. High strain rate experiments were carried out on Split Hopkinson Pressure Bar (SHPB). Plastic stress wave propagation, dynamic effects and non-uniform deformation of the specimen, not taken into account by Kolsky analysis of the SHPB, were investigated numerically by Finite Volume Method (FVM). Three different testing temperatures were selected. Results, in terms of flow stress at 5% of plastic strain indicate rather low strain rate sensitivity, with a tendency of negative strain rate sensitivity at lower temperatures at very high strain rates above 2000 strains per second. The metallographic examination carried out on the 7xxx series alloy showed that this drop in flow stress may be related to strain localisation.

Keywords: *high strain rate, finite volume simulation, extrusion, microstructural evolution*

1. INTRODUCTION

Processing and manufacturing of metal products involve deformation, where the strain rate may vary from magnitudes which are typical for creep (10^{-8}-10^{-5} s^{-1}) to orders of magnitude higher (10^{3}-10^{4} s^{-1}). Much attention has been paid to the quasistatic and intermediate strain rate regime, less than about 50-100 s^{-1}, in order to relate variations in strain rate to flow stress, deformation microstructure and texture, as well as the effect of strain rate on the subsequent annealing response in terms of the recrystallisation microstructure and texture [1,2]. In the case of the high strain rate regime, higher than 100 s^{-1}, remarkably little research has been directed to correlate microstructural evolution as a function of variations of strain rate. This fact can be related to the lack or less accessibility to experimental test facilities which can handle high strain rates in a controlled manner. However, the Split Hopkinson Pressure Bar (SHPB) equipment, originally proposed by Kolsky [3] and since then constantly being developed [4,5], can handle strain rates to several thousands per second. However, the so-called Kolsky analysis does not take the inertia effects and plastic stress wave propagation into account. Following considerations in [6], Finite Volume Method (FVM) has been selected to numerically correct the experimental results obtained on the SHPB.

Since industrial operations such as high speed machining, friction stir welding and extrusion often involve high strain rate of deformation in some areas of the product, it is important to gain the knowledge of the high strain rate behaviour and the microstructural evolution and whether it is in a line with the predictions obtained from quasistatic and intermediate strain rate regions.

2. INDUSTRIAL EXAMPLE OF HIGH STRAIN RATE PHENOMENON

An example from extrusion of an aluminium alloy (6xxx series alloy) will now be presented in order to demonstrate the importance of strain rate on microstructure and texture evolution (for

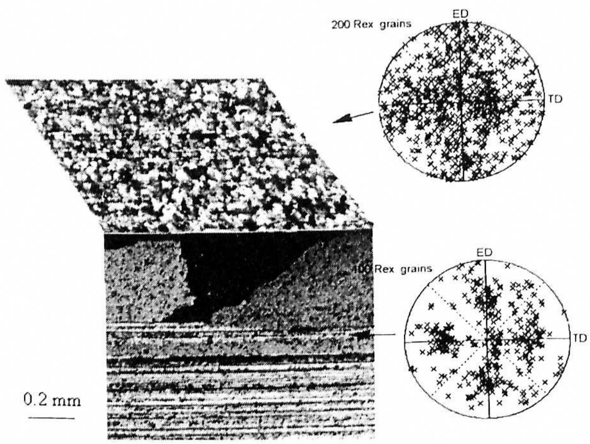

details, see [7]). The micrograph in Figure 1 shows the grain structure of an aluminium profile deformed with a ram speed of 25 mm/s (which is often used in industrial extrusion). It has been shown [7] that such a ram speed gives strain rates as high as 3000 s^{-1} at the very surface of the profile. The strain rate gradient is very steep at the surface and decreases very fast to less than 100 s^{-1}. In the centre of the profile the strain rate is less than $10s^{-1}$.

Fig.1. Microstructure in longitudinal and extrusion plane sections and (111) pole figures showing the texture at different positions of the profile

Figure 1 shows that at the very surface, the grain structure is equiaxed with a grain size less than 20 μm, whilst only about a grain layer below this surface structure, the grain structure changes quite dramatically into elongated grains and a grain size more than an order of magnitude larger than at the very surface. Another interesting difference is the texture at two locations. The {111} pole figures (measured by EBSP) taken from both the surface, close to the surface and in the centre region depict very different grain orientations. The small grain size area has a more or less random texture, which is often associated with particle stimulated nucleation of recrystallisation. The close to surface area has a relatively sharp 45° rotated cube texture, which can be associated with nucleation from pre-existing grain boundaries in a region with a shear texture. The centre region (not shown above) depicts a strong cube texture which is a typical recrystallisation texture for plane strain deformation conditions. The present case demonstrates that the strain rate affects the texture, recrystallised grain size and nucleation mechanisms to a really large extent. Extrusion is an important industrial process, thus the need to increase the understanding of the effect of high strain rate on deformation behaviour.

3. EXPERIMENTAL PROCEDURE

Two commercial aluminium alloys of 6xxx and 7xxx series, cast and homogenised using standard industrial practise and with the chemical composition given in Table 1 were tested over the wide range of strain rates from 0.1 to over 3000 strains per second. Three different characteristic temperatures were chosen: room, temperature near solvus of characteristic hardening precipitates and between those two, where the rate of growth of coherent particles is reaching the maximum.

Element	Si	Fe	Cu	Mn	Mg	Zn	Ti	Ga	Zr	Ni	Cr	Base	Other
6xxx	0.973	0.192	0.014	0.556	0.606	0.006	0.010	0.018	0.001	0.001	0.002	97.615	<0.0015
7xxx	0.079	0.141	0.014	0.010	0.863	5.450	0.015	0.014	0.183	0.004	0.001	93.210	<0.0015

Table 1. Chemical composition (in wt%) of investigated alloys

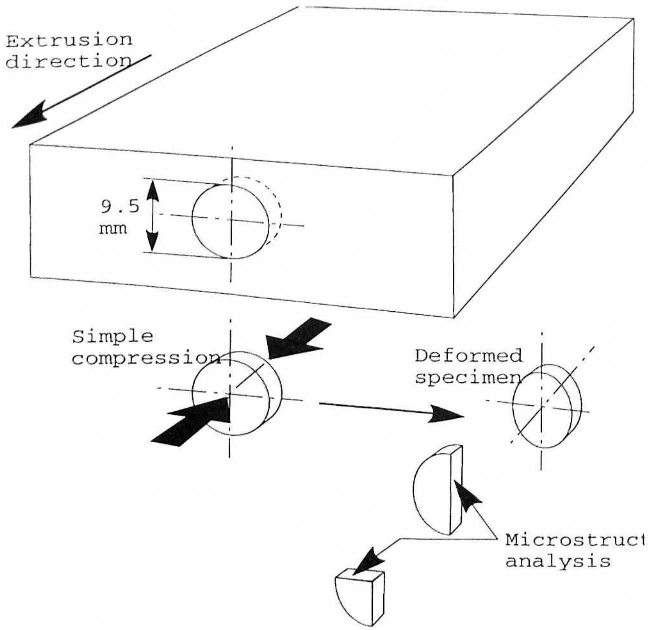

Specimens of cylindrical shape of 9.5 to 10 mm diameter nominally, were cut from flat extruded sections and tested in uniaxial compression, so the axis of deformation was parallel to the extrusion direction as shown on Fig.2. Both alloys were in tempered condition, peak aged, T6, for 6xxx and overaged, T79, for 7xxx series alloy. Intermediate testing from 0.1 to 100 strains per second has been carried out using a computer controlled servo-hydraulic testing machine. Specimen were 7.5mm thick.

Fig.2. Schematic of specimen geometry

Testing at strain rates higher than 500 strains per second was performed using SHPB. The principle of SHPB testing allows for stress wave propagation effects by applying the one-dimensional elastic wave propagation theory. Specimen is placed between two long bars: incident and transmitted. Gas gun driven projectile creates an impact at the end of the incident bar, thus generating the stress wave, which propagates along the incident bar. Upon reaching the incident bar-specimen interface this wave is partially reflected and partially transmitted. All signals: incident, reflected and transmitted are recorded by strain gauges placed at the bars. Assuming uniform deformation of the specimen and no dynamic effects stress-strain curve is calculated from the recorded signals.

However, the assumptions can lead to wrong results as the inertia forces and plastic stress wave propagation can not be neglected [6], so numerical correction was performed. To obtain the stress-strain curve, which does represent inherent material property, specimens of two different nominal thicknesses 4.5mm and 2.5mm were used. Numerical procedure was continued iteratively, until stress-strain curve identical for both geometries is reached. A detailed description of the method used and the numerical formulation of the problem can be found in [8].

4. RESULTS AND DISCUSSION

4.1. Mechanical properties

Stress-strain curves were plotted for all tests performed and strain rate sensitivity was assessed by plotting of true stress at constant plastic strain of 5% vs strain rate in semi-logarithm scale. The reason for choosing 5% of plastic strain is two-fold.

Firstly, steady state flow stress is more difficult to reach at higher strain rates, due to reduced dynamic recovery. The strain at the saturation stress is expected to be very large. Strain attainable by the SHPB is a dependent parameter. Since it is "produced" by impact, total strain is related to the geometry of the projectile and its velocity at impact, i.e. the kinetic energy of the projectile at impact. This implies that lowering the velocity of the projectile to test at lower rates will result in lower strains, so the length of the projectile had to be increased. However, there is an upper bound in the length of the projectile, since it is driven by a gas gun. To meet both requirements, 5% of plastic strain was chosen as the optimum.

Secondly, constant strain rate in SHPB is maintained only within the effective duration of the reflected strain signal and 5% of plastic strain was satisfactory in most experiments.

The results for 6xxx in T6 and 7xxx in T79 condition are shown on Figures 3. and 4. Results at strain rates higher than 1000 are numerically corrected ones and represent the real response of the material. Both alloys indicate low strain rate sensitivity which increases with the increase of temperature. The low strain rate sensitivity of aluminium alloys in tempered condition is not surprising and is in a good agreement with the results reported on alloys of same series tested in the same condition [9].

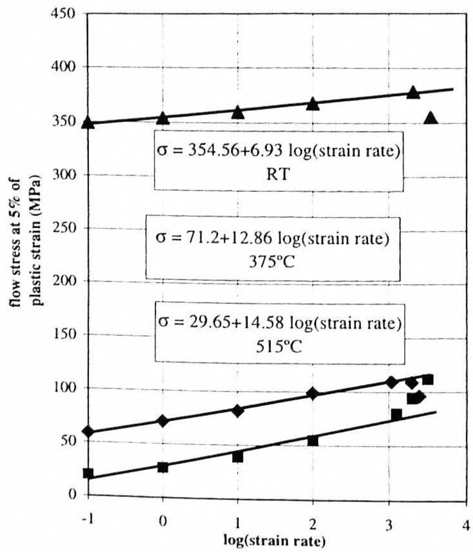

Fig.3. Flow stress vs logarithm of strain rate at three different temperatures for 6xxx

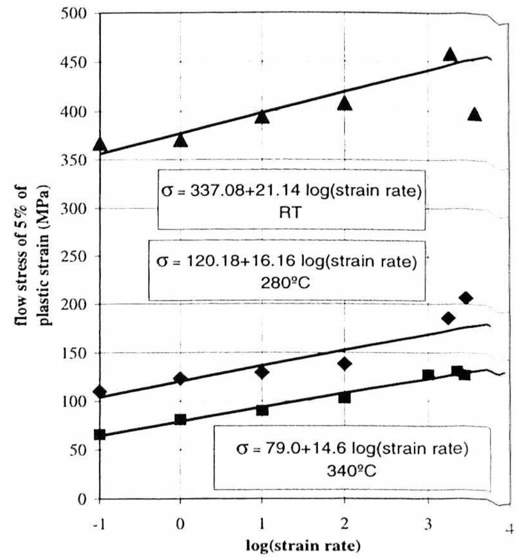

Fig.4. Flow stress vs logarithm of strain rate at three different temperatures for 7xxx

However, it is interesting to observe an obvious change in the trend above 2000 strains per second at lower temperatures for both alloys. At these strain rates, it is seen that the flow stress drops more than 50 MPa for the 7xxx series alloy, whilst it is somewhat less for the 6xxx series alloy. Such a drop in flow stress may occur if strain localisation such as shear banding or deformation bands appear. The tendency of a material to deform inhomogeneously is reflected in the strain rate sensitivity parameter m; materials with negative and small values of m (such as non-heat-treatable Al-Mg alloys, where Mg appears in solid solution) are more susceptible to inhomogeneous deformation compared to materials with higher m-values. At higher deformation temperatures, the recovery processes occur much faster than at room temperature. Thus, more slip planes are activated through increased activity of cross-slip reactions and climb of dislocations leading to more homogenous deformation.

For the 7xxx series alloy the m-values of 0.022, 0.049 and 0.065 for room temperature, 280°C and 340°C respectively were obtained. For the 6xxx series alloy the m-values were 0.008, 0.064 and 0.148 for room temperature, 375°C and 515°C, respectively. The significantly lower m-value at room temperature for both alloys indicates a higher tendency to strain localisation at low temperatures than at higher temperatures. In all cases the m-values are obtained by fitting the power law through those points which are in a good agreement with the trend. This was done in order to emphasise the departure from the trend at very high strain rates.

4.2. Metallographic examination

In order to give an explanation of the drop in flow stress at high strain rates metallographic examinations were carried out. Examination focused on the 7xxx series alloy, which gave the largest drop in flow stress. For the SHPB tests the micrographs are taken at a higher deformation ratio than where the flow stress was recorded, however, we believe that the drop in flow stress is maintained for all strains at the actual strain rate.

The microstructure of the extruded material, which was the starting point for the SHPB-testing (see Fig.2), is shown in Fig.5. The material is non-recrystallised and consist of highly elongated grains in the longitudinal transverse section, less elongated grains in the extrusion plane and more equiaxed grain in the short transverse section. The micrographs shown in Fig.6 are both taken in the extrusion plane. In Fig.6(a) the grain structure after SHPB-testing at room temperature to a reduction of 39% using strain rate of approximately 4000 s^{-1} (3996 s^{-1}) is revealed.

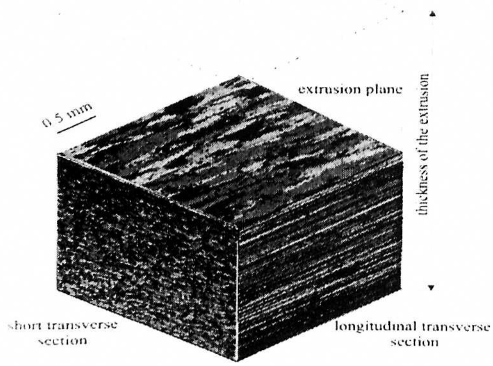

Fig.5. Microstructure of the as-extruded material

Fig.6(b) shows the microstructure in as extruded condition using the same magnification as in Fig.6(a). From these two micrographs, it is quite clear that the original grain structure has changed due to the high strain rate of deformation. The original grain boundaries have bulged/moved perpendicular to the extrusion and the compression direction and the distance between the grain boundaries has increased. Since the deformation is parallel to the fiber structure, it is expected that the boundaries will bulge normal to the deformation direction. Corresponding observations were also made at the higher deformation temperatures (280 and 340°C).

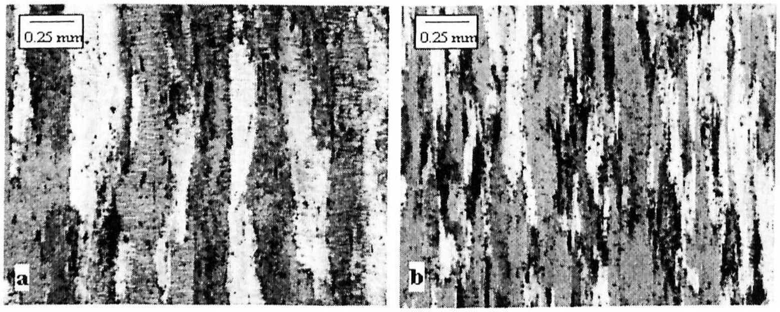

Fig.6 Optical micrographs taken in the extrusion plane revealing microstructure of (a) SHPB tested (b) as extruded

However, more interesting are the parallel bands normal to the compression direction. The deformation bands are seen to be normal to the compression direction in all grains irrespective of the different grain orientations. Scanning electron microscopy equipped with an EBSP-unit was applied in order to study whether these bands were of a high or a low angle character. From those investigations it was quite clear that the microstructure inside the grains consisted of boundaries less than 15°; i.e. low angle boundaries.

In order to study these observations in more detail, the material in Fig.6(a) was analysed by transmission electron microscopy and TEM micrograph of the SHPB tested material, from the same area and plane as Figure 6(a) is shown in Figure 7. The sample taken from the as-extruded material, displays a homogeneous substructure with a subgrain size of 5μm. The sample deformed 39% by SHPB shows a microstructure which is totally different as compared to the extruded material.

Fig.7. TEM of the sample deformed 39% at $3996s^{-1}$

The structure is rather inhomogeneous and consist of microbands with sharp dislocation walls aligned in the same direction. In between these microbands the structure consists of individual dislocations with a relatively high density. The subgrain boundaries from the as extruded condition are completely removed. As pointed out above, the drop in flow stress may be linked to strain localisation and the micrograph in Figure 7 confirms this statement.

5. CONCLUDING REMARKS

The results obtained in the present work show that both alloys, in terms of flow stress at 5% of plastic strain, possess rather low strain rate sensitivity, with a tendency of negative strain rate sensitivity at room temperature at very high strain rates above 2000 strains per second. The metallographic examination carried out on the 7xxx series alloy showed that this drop in flow stress may be related to strain localisation. Work is in progress to analyse structures deformed at higher temperatures and high strain rates and the effect of the observed inhomogeneous microstructures on recrystallisation structure and texture.

6. REFERENCES

[1] K. D. Vernon-Parry, T. Furu, D. J. Jensen and F. J. Humphreys: Mat. Sci. Tech., 12 (1996), 889.
[2] R. K. Bolingbroke, T. Furu, D. J. Jensen and K. Vernon-Parry: Mat. Sci. Tech., 12 (1996), 897.
[3] H. Kolsky: Proc. Phys. Soc. London, B62 (1949), 676.
[4] S. K. Samanta: J. Mech. Phys. Solids, 19 (1971), 117.
[5] D. A. Gorham: J. Phys. D: Appl. Phys., 22 (1989), 1888.
[6] N. N. Dioh, A. Ivankovic, P. S. Leevers and J. G. Williams: Proc. R. Soc. London, A449 (1995), 187.
[7] T. Furu, Ø. Sødahl, E. Nes, L. Hanssen and O. Lohne, Mat. Sci. Forum, 157-162 (1994), 1197.
[8] L. Djapic Oosterkamp, A. Ivankovic and G. Venizelos: submitted to Mat. Sci. Eng. A.
[9] D. L. Holt, S. G. Babcock, S. J. Green and J. Maiden: Trans. ASM, 60 (1967), 152.